Wearable Motion Sensing Glove

24-673: Project Report

Team Members: Mehar Singh, Esther (Jae-Eun) Lim

Background:

Understanding the interactions with our external world has increasingly become important in the field of robotics – as it allows us to recognize and manipulate objects with high accuracy and dexterity. These ideas have been studied intensely in robotic disciplines such as Motion Planning and Computer Vision to identify the intention and control of humans. However, the emerging fields of Human-Computer Interaction and Soft Robotics can be applied to gain a better understanding of motion detection – through wearable electronic sensors.

However, the multitude of these devices that have been developed since the 1970s both for research and commercial applications have met with various challenges and limitations – in that it is not easy to manufacture an inexpensive solution to detect hand and arm motions. Current technologies have yielded devices with low accuracy and poor user-friendliness [1]. While, traditional methods for motion detection use computer-vision based optical sensors that are bulky and hard to integrate within soft structures, emerging technologies in wearable computing have the potential to achieve these low-cost sensing materials with relatively high accuracy and reliability.

Introduction:

Emerging fields in wearable electronics and artificial skin have the potential to better interface human-robot interactions. However, in order to effectively use these technologies to its fullest degree, we must work on overcoming the accuracy and design challenges associated with these products.

The objective of this research is to create a design using wearable electronics to fabricate a wearable motion sensing glove to overcome the accuracy challenges associated with commercial products. The research also focuses on the modelling of the bend sensors – that were used in the design – primarily to account for sources of error that cause extra resistance in the sensor. These errors are primarily caused by the pressure under the sensor. The modelling of the pressure effect is our major contribution as there is a large gap in the modeling of these bend sensors and errors in commercial applications of these technologies.

Design Implementation

Our proposed solution is to explore the field of wearable electronics to accomplish this purpose for the wearable athletic device. The design that we implemented was a latex glove with bend sensors – for strain sensing – to give us motion detection for sport and other activities. This design implementation is beneficial as the detection system is more compact, lightweight and convenient to use than its predecessors. Our bend sensor measured its stretch and reported an associated resistance with the corresponding stretch. We used an Arduino to interpret the resistances and map it with our measured angle.

We can then analyze and display the data and movements on a graph to showcase the person's movements. The motivation behind this is to compare the form and movement to that of an 'idealized' form that can enable athletes and users to improve their motions. For example, if the user is shooting a basketball, we can compare the shooting motion to that of a professional athlete so that they can better their ability to shoot the basketball.

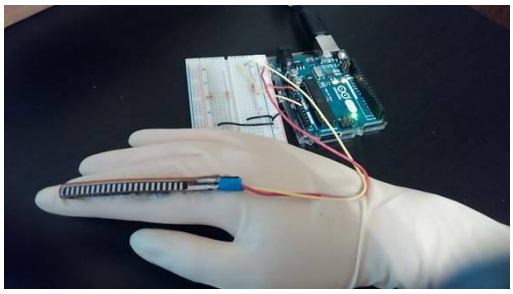

Figure 1 – Glove Design

Modeling and Simulation

We have modeled our bend sensor as a simple cantilever beam. Moreover, we extended our model to account for the pressure effect that is prevalent while using the glove. The pressure effect arises as a result of the knuckle pressing up against the flex sensor at the bending point – which can cause errors and uncertainties in our measurements. Through the modeling of the error, we seek to improve accuracy for our design and contribute to the modeling work done in the field of wearable electronics.

Methodology

Our approach to this project consists of two main aspects – the design of the glove and modelling of the commercial flex sensor. Our focus is primarily on the modeling of the errors in the glove for this report.

In the design of the motion sensing glove – we used a latex glove with a commercial flex sensor that was attached to the index finger. The latex glove was used as it has a similar modulus of elasticity to our skin. The flex sensor was then connected to an Arduino that was used to calibrate the sensor to prevent drift and relate the stretch and resistance readings of our sensor into our angle measurement. We modeled our flex sensor as a simple cantilever beam. The manufacturer's specifications indicated that there was a linear fit between the electrical resistance output and the angle of the flex sensor. This ranged from 10kΩ to 110kΩ. However, in our design, we found that our resistance output ranged from 30kΩ to 90kΩ. Thus, we calibrated our output accordingly.

With the motion sensing capabilities in place, we conducted preliminary experimental validation on our sensor, in order to determine the empirical mapping between the electrical resistance and bend angle of our finger. We varied the angle of the flex sensor by bending our finger and measuring the output resistance and mapped angle. The finger was bent from 0^o to approximately 90^o and repeated over 5 trials. In order to determine the 'actual' angle associated with our finger, we used the image processing software – ImageJ – to measure the bent angle of our finger. We ran the ImageJ software 5 times over each image to determine the angle of our finger to reduce errors associated with the image processing. This allowed us to visualize and plot the measured experimental and actual angles of our finger (shown in Figure 6 below). Using this data, we were able to determine a correlation between the measured resistance of the flex sensor and the corresponding angles (both experimental and actual). We were then able to determine the error as a function of our bend angle of our finger in order to determine possible sources of error and their modeling.

Below is our list of possible causes of error and our analysis on each:

Possible Sources of Error:

1. **Pressure Effects** - As the finger bends, the knuckle presses against the sensor and causes it to stretch more. This stretch can increase the resistance.
2. **Buckling** - Buckling may cause extra bending of the sensor beyond the bend angle of the finger.
3. **Viscoelasticity** – Due to friction between the glove and the skin, the motion of the sensor may be delayed.
4. **Hysteresis** - Hysteresis is another possible source that could introduce unwanted offset to our measurements.

However, through our experimentation and analysis, we found that the pressure effect was the dominant source of error. A visual inspection of our flex sensor mounted on our hand at all angles indicated that there was no buckling

present in the sensor. Moreover, to ensure that viscoelastic effects were negligible we took our measurements at steady state and waited for our resistance values of the sensor to stabilize. Hysteresis was also neglected in our modeling as our measurements were consistent regardless of the repeated bending motion of the finger.

Theory and Modeling

Cantilever Beam

We modeled our bend sensor as a simple cantilever beam that was fixed at the center (the bending point of the sensor) to determine the bend angle based on the force applied to the end of the finger to cause it to bend. This model is shown below in Figure 2:

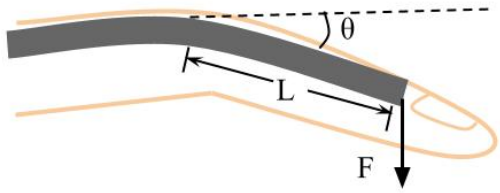

Figure 2 - Simple Cantilever Beam Model of Flex Sensor

Figure 2 shows the flex sensor attached to the index finger with its center at the finger joint. When bending the finger, the flex sensor bends about the joint. A force, F, is applied at the end of the sensor near the fingernail as the finger bends. The bend angle, θ, of the flex sensor due to the applied force is obtained from the following equation:

$$\theta = \frac{FL^2}{2EI} \tag{1}$$

Where L is half of the length of the flex sensor, or the distance from the bending point to the end where force is applied and E is the modulus of elasticity of the bend sensor. The moment of inertia, I, is determined by the following equation, assuming the flex sensor has a rectangular cross section:

$$I = \frac{wt^3}{12} \tag{2}$$

Where t is the thickness of the flex sensor and w is the width of the flex sensor as shown in Figure 3.

Figure 3 – Cross Section of Flex Sensor

Therefore, with the calculated angle, we can relate it to the resistance of the sensor to determine the model.

Bending Effects

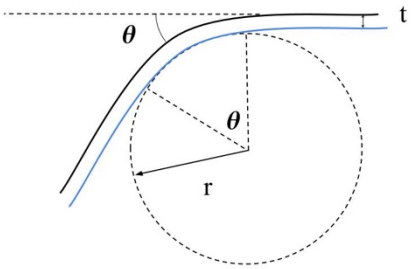

Figure 4: Bending model diagram

As the finger bends, the sensor is stretched, which is detected as change in resistance. To model the relationship between resistance and bend angle, we first consider the relationship between elongation and bend angle. The blue line in Figure 4 represents the neutral axis of bending and the black line represents the sensor. Since the sensor is offset from the neutral axis by thickness, t, the sensor stretches with increasing bend angle.

When the sensor bends, the middle section of the sensor forms an arc while the adjacent sections remain nearly straight. Hence, we assume that the elongation outside of the arc is negligible and only consider the elongation within the arc.

The arc length of the neutral axis at an arbitrary bend angle, θ, is given by Equation 3:

$$l_0 = r\theta \tag{3}$$

where r is the radius of the arc. The arc length of the sensor at θ is given by Equation 4:

$$l = (r + t)\theta \tag{4}$$

Note that the length of the neutral axis does not change. Therefore, it represents the length of the sensor before elongation. To find the elongation, we take the difference between the arc length of the neutral axis and the sensor at θ:

$$\Delta l = l - l_o = t\theta \tag{5}$$

Next, we modeled the resistance due to bending as the change in resistance due to elongation:

$$\Delta R = \frac{\rho \Delta l}{A_c} \tag{6}$$

where ρ is the resistivity of the sensor and A_c is the cross-sectional area of the sensor. If we plug Equation 5 into Equation 6, we get:

$$R_{bending} = \frac{\rho t\theta}{A_c} \tag{7}$$

From the sensor reading which was programmed to map the resistance to bend angle based on manufacturer specification, we found the mathematical relationship between resistance and bend angle:

$$R_{bending} = 581\theta + 31{,}130\ \Omega \tag{8}$$

From Equation 6, we have that $\rho t/A_c = 581\ \Omega/\text{degree}$. Since the resistance does not start from zero at a zero-degree bend angle, we have taken into account the constant as well. Hence, Equation 8 represents our final bending model.

Pressure Effects

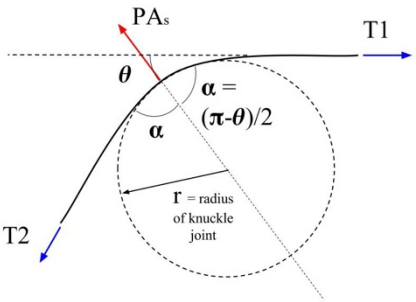

Figure 5: Pressure model diagram

As the finger bends, the sensor is pressed against the knuckle of the finger. This causes change in pressure with change in bend angle. The change in pressure in turn elongates the sensor which causes further change in resistance. To account for this, we also model the effect of pressure on resistance.

First, we consider the tensile force along the sensor formed due to pressure. In Figure 5, the blue arrows represent tensile forces that counteracts the pressure shown in red arrow. Based on force balance, the following relationship between the two tensile forces is made:

$$T_1 \sin(\alpha) = T_2 \sin(\alpha) \tag{9}$$

This leads to $T_1 = T_2 = T$. The force balance along the pressure gives us the following:

$$T_1 \cos(\alpha) + T_2 \cos(\alpha) = 2T \cos(\alpha) = PA_s \tag{10}$$

where $A_s = wr\theta$ is the contact area on which the pressure is applied (w is the width of the sensor). Solving for the tensile force, we get:

$$T = \frac{PA_s}{2\cos(\alpha)} \tag{11}$$

We now consider the elongation of the sensor due to the tensile force which is given by Equation 12:

$$\Delta L = \frac{TL_o}{EA_c} \tag{12}$$

where L_o is the unstretched length of the sensor, E is the elastic modulus of the sensor, and A_c is the cross-sectional area of the sensor. Using the similar process we used to derive the bending model, we plug in Equation 12 to Equation 7 to get the pressure model:

$$R_{\text{pressure}} = \Delta R = \frac{\rho \Delta L}{A_c} = \frac{\rho r}{EA_c{}^2} \frac{L_o w}{2} p \frac{\theta}{\cos\left(\frac{\pi - \theta}{2}\right)} \tag{13}$$

From the pressure experiment, we got the equation $\theta = 4.342p$ degree, ignoring the constant. Solving for the pressure we get $p = 0.2303\theta$ psi. Then we plug this equation into Equation 11 and let $\frac{\rho r}{EA_c{}^2}\frac{L_o w}{2} = k$. To solve for k, we considered Equation 19, which gives us that $R = 11{,}700\ \Omega$ at $\theta = 20°$. Plugging in this pair of values, we get at $k = 1.3$ which gives us the following equation for the pressure model:

$$R_{pressure} = 1.3\frac{0.2303\theta^2}{\cos\left(\frac{\pi - \theta}{2}\right)} \tag{14}$$

Results & Discussion

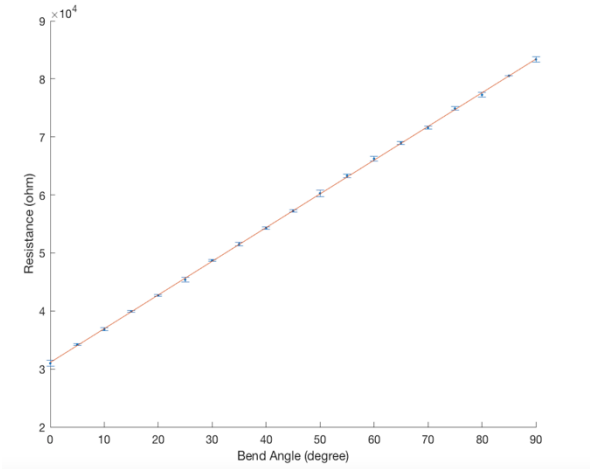

Figure 6: Resistance versus Bend Angle

For the first project review, we collected experimental data of the sensor reading of the resistance and bend angle. We programmed the Arduino to map the resistance to bend angle based on manufacturer specification. For a 5° increment, from 0° to 90°, we measured the resistance five times and plotted the mean with the uncertainties in Figure 6. The plot shows the relationship between the resistance and the corresponding bend angle in the case that the change in resistance is purely due to bending.

A linear fit of the plot gives the following equation, which describes the relationship between resistance and bend angle:

$$R = 581\theta + 31{,}130\ \Omega \tag{15}$$

For the second project review, we improved our experiment setup to make more accurate and consistent measurements. We used Velcro to attach the sensor to the index finger and soldered the wires to the sensor. We took profile pictures of the finger bending in approximately 10° increment, from 0° to 90° (Figure 9) and recorded the sensor readings of the resistance and angle. During the experiment, the hand was rested on a flat platform.

After the measurement, we used ImageJ to get the actual bend angles of the finger. We repeated this procedure five times and plotted the mean actual angle and the uncertainties. Figure 7 shows the measured angle and the actual angle corresponding to the resistance readings. The linear fit for measured angle and resistance is given by the following equation:

$$R_{measured} = 577.9\ \theta + 31{,}250\ \Omega \tag{16}$$

The linear fit for actual angle and resistance is given by the following equation:

$$R_{actual} = 587.1\ \theta + 34{,}400\ \Omega \tag{17}$$

Figure 8 shows the error between the actual and measured angle. The linear fit of the error in resistance is given by the following equation:

$$R_{error} = 9.2\ \theta + 3{,}150\ \Omega \tag{18}$$

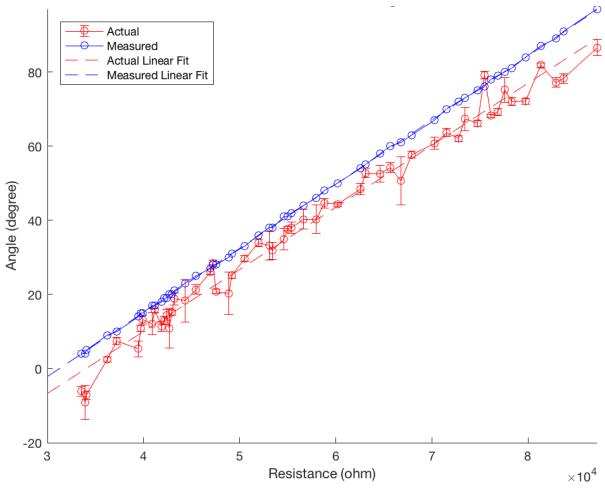

Figure 7 – Measured and Actual Resistance vs Angle

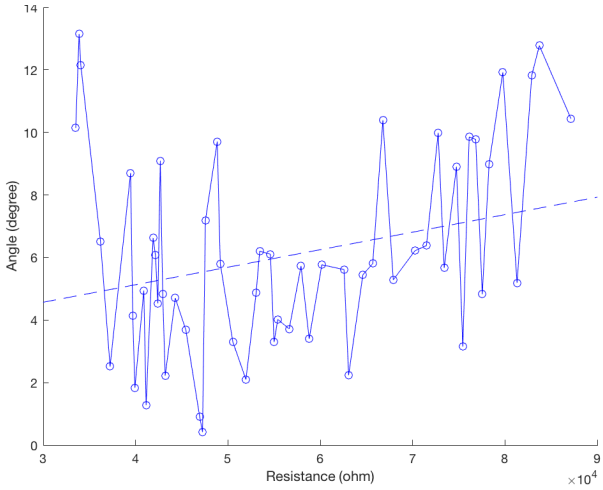

Figure 8 – Error of measured resistance

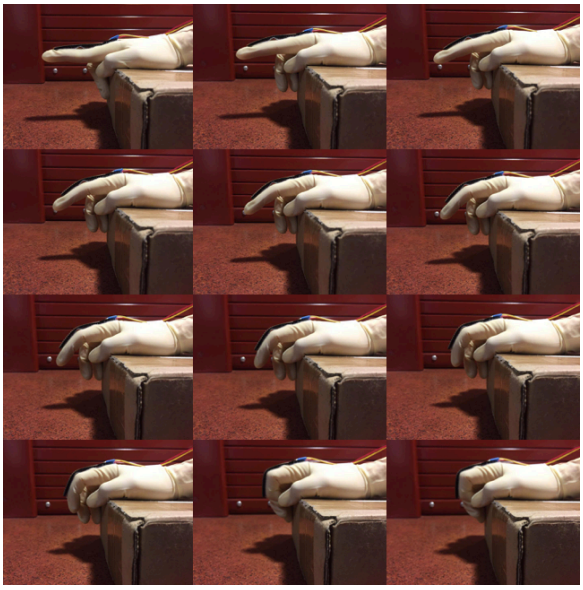

Figure 9 – Incremental Bending of Finger (One Trial)

To make a more accurate model of the relationship between pressure and bend angle and resistance, we re-gathered data from experiment. We used four weights (200g, 100g, 50g, 20g) and a foam pad with a width of 0.2 inches attached to the bottom of the weights to create uniform contact area with the sensor. Since the sensor has a width of 0.25 inches, the contact area to which the weights were applied was $A_s = 0.05\ in^2$. We placed the sensor with the ends resting on two wooden boards so that the center of the sensor was hanging (Figure 10). With weights applied to the center, the sensor was allowed to bend naturally.

We did not fix the ends of the sensor to reduce possible measurement errors due to extraneous forces. The weights were lowered freely with a string so that no force from the hand was transmitted to the sensor. For each weight, we made the measurements five times and plotted the mean and the uncertainties.

Figures 11 and 12 show the results from the experiment. With linear fit, the relationship between pressure and bend angle is $\theta = 4.342p + 25.39$ degree, and the relationship between pressure and resistance is $R = 2540p + 45{,}880\ \Omega$. Both show positive relationship.

Since we care about the change in bend angle and resistance due to change in pressure, we only consider the slopes. We neglect the constants of the equations, which may introduce errors due to imperfect initial condition of the sensor.

Combining both equations while neglecting the constants we obtain the following relationship between resistance and angle due to pressure:

$$R_{pressure} = 585\theta\ \Omega \tag{19}$$

Figure 10: Pressure experiment setup

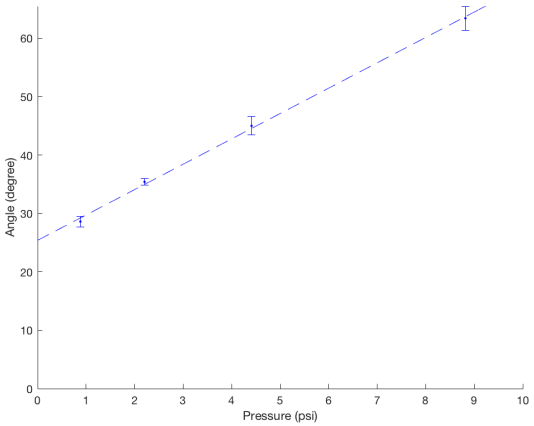

Figure 11: Pressure effect on angle

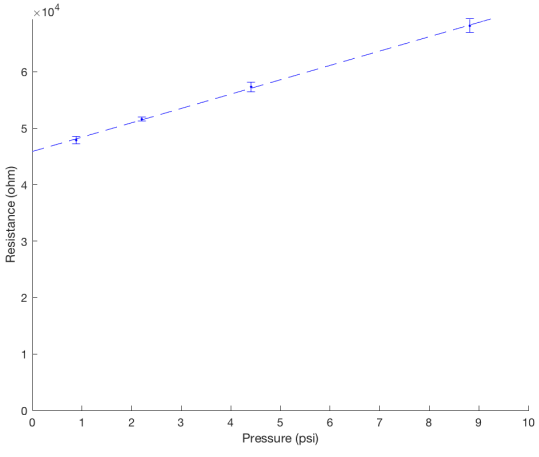

Figure 12: Pressure effect on resistance

Final Model

The final model that maps the resistance with the actual bend angle of the finger is obtained by adding the resistance purely due to bend angle and the resistance due to pressure:

$$R_{total} = R_{bending} + R_{pressure}$$

$$R_{total} = 581\theta + 31{,}130 + 1.3\frac{0.2303\theta^2}{\cos\left(\frac{\pi - \theta}{2}\right)}\ \Omega \tag{20}$$

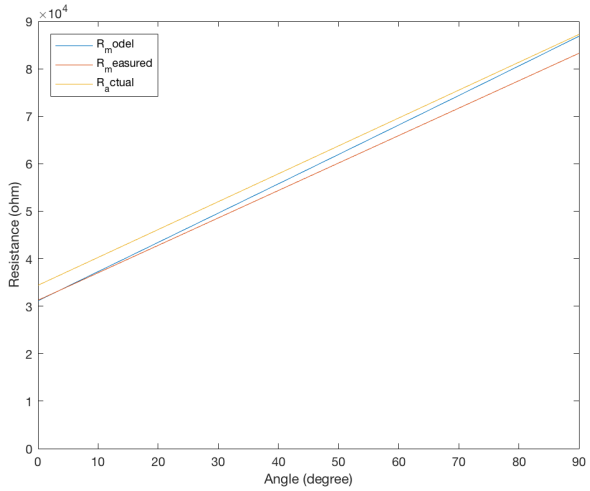

Figure 13: Comparison between the model and measured and actual values

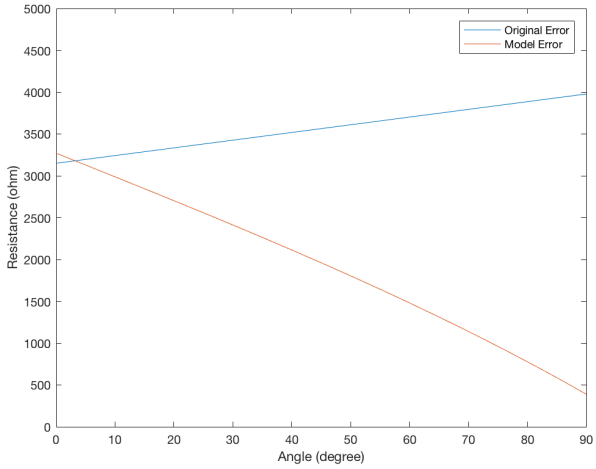

Figure 14: Comparison between original error and model error

Figure 13 shows the plot of the pressure model (Equation 20) in blue. The measured resistance is plotted in red and the actual resistance is plotted in yellow. Since the pressure is zero at 0° and increases with bend angle, the plot shows the pressure model approaching the actual resistance with increasing angle.

Figure 14 compares the error of the original measurement (Equation 21) and the pressure model (Equation 22). It is clear that the model error decreases with increasing angle whereas the measurement error increases with increasing angle.

$$E_{measured} = 9.2\theta + 3150\ \Omega \tag{21}$$

$$E_{model} = 6.1\theta + 3270 - 1.3\frac{0.2303\theta^2}{\cos\left(\frac{\pi - \theta}{2}\right)}\ \Omega \tag{22}$$

For smaller angles, there is still a gap between the model and the actual resistance. The source of error must be more dominant for small angles. It may be due to the combined effect of the sources of error listed in Error Analysis section. Nevertheless, the error due to pressure accounts for approximately half of the error in the measurement, which significantly improves our final model.

Conclusion

Summary

In our project, we implemented a system design that maps out our joint angle as a function of resistance. We accomplished this by using a flex sensor that outputs resistance as it stretches and bends. We mounted this on a glove on top of our index finger to map out the motion of our finger. From our results, we found there was a discrepancy between our measured and actual angle. After some experimentation, we found out that the pressure effect was a major cause of this error.

We modeled this error and bending effects to determine a mathematical model of our flex sensor in order to better determine how it operates. With our model, we empirically determined the geometric and material constants of our flex sensor in order to plot our theoretical model vs the actual model we obtained. Our theoretical model, incorporating our errors (pressure effects), reduced our error by approximately 50%. This validated our experimental results of the pressure effect being a major cause of the error.

Future Work

Our future work hopes to further our theoretical modeling and design implementation of our glove. We would like to focus on improvements in the modeling of our error effects. In our model, we accounted for approximately half of the errors observed in our model. We would like to focus on other potential effects and attempt to model them to further increase our accuracy of our flex sensor. Moreover, we would like to add features to our current existing design. Our goal is to map out hand movements as a function of time in a highly dynamic environment in order to be used in real world applications such as technique monitoring in sports.

References

[1] Park, Y.L., Chen, B.R. and Wood, R.J., 2012. Design and fabrication of soft artificial skin using embedded microchannels and liquid conductors. IEEE Sensors Journal, 12(8), pp.2711-2718.

[2] Park, Y.L., Majidi, C., Kramer, R., Bérard, P. and Wood, R.J., 2010. Hyperelastic pressure sensing with a liquid-embedded elastomer. Journal of Micromechanics and Microengineering, 20(12), p.125029

[3] Chossat, J.B., Park, Y.L., Wood, R.J. and Duchaine, V., 2013. A soft strain sensor based on ionic and metal liquids. IEEE Sensors Journal, 13(9), pp.3405-3414.

[4] Majidi, C., Kramer, R. and Wood, R.J., 2011. A non-differential elastomer curvature sensor for softer-than-skin electronics. Smart Materials and Structures, 20(10), p.105017.

[5] Amjadi, M., Pichitpajongkit, A., Lee, S., Ryu, S. and Park, I., 2014. Highly stretchable and sensitive strain sensor based on silver nanowire–elastomer nanocomposite. ACS nano, 8(5), pp.5154-5163.